

Estimating the uncertainty in passive-microwave rain retrievals

Dorothee Coppens, Ziad S. Haddad and Eastwood Im

Jet Propulsion Laboratory, California Institute of Technology, Pasadena, CA 91106 – e-mail : dorothee@AlbertoVO5.jpl.nasa.gov

Abstract

Current passive-microwave rain-retrieval methods are largely based on databases built off-line using cloud models. Because the vertical distribution of hydrometeors within the cloud has a large impact on upwelling brightness temperatures ([6],[7]), a forward radiative transfer model can associate microwave radiances with different rain scenarios. Then, to estimate the rain from measured brightness temperatures, one looks for the rain scenarios in the database whose associated radiances are closest to the measurements. To understand the uncertainties in this process, we analyze the marginal and joint distributions of the radiances observed by the Tropical Rainfall Measuring Mission (TRMM) satellite's passive microwave imager, and of those in the databases used in the TRMM passive rain retrieval. We also calculate the covariances of the rain profiles and brightness temperatures in the TRMM passive-microwave database and derive a simple parametric model for the conditional variance, given measured radiances. These results are used to characterize the uncertainty inherent in the passive-microwave retrieval.

Keywords

Passive-microwave, estimation, rainfall distribution, TRMM mission.

I. INTRODUCTION

MOST instantaneous passive microwave rain retrieval algorithms currently implemented use a cloud database constructed off-line. The database associates calculated microwave brightness temperatures to sample rain events representing those that are expected to produce the eventual measurements. Once the database is constructed, one processes each set of instantaneous measurements by searching the database for those scenarios whose associated radiances are closest to the measurements. The details of the search and eventual estimation procedures differ from one retrieval algorithm to the other, but the general principle is the same. In the case of the Tropical Rainfall Measuring Mission's Microwave Imager (TMI), the passive-microwave instantaneous retrieval algorithm uses a large database which was constructed using various cloud models simulations. Radiative transfer calculations followed by the appropriate filters were used to associate to each simulated rain event (itself consisting of surface wind and temperature, and relative humidity and hydrometeor profiles) the brightness temperatures which one would expect the TMI's 10.7 GHz H- and V-pol, 19.3 GHz H- and V-pol, 22.2 GHz V-pol, 37 GHz H- and V-pol, and 85.5 GHz H- and V-pol channels to measure.

Given a set of measured radiances, one hardly ever expects to find in one's database exactly matching calculated brightness temperatures. It is therefore important to be able to estimate the "spread" of the closest near-matches that one does find. To quantify this uncertainty, we start by studying the joint behavior of the brightness temperatures and of the rain in the vertically layered atmosphere. The results are used to quantify the conditional variance of the estimated rain given a set of microwave radiances. They are also used to compute the conditional covariance of the brightness temperatures given the rain, as knowledge of this covariance is crucial to those retrieval algorithms such as the currently implemented TMI's ([2]), which rely on Bayes's re-formulation of the desired probability $p(\vec{R}|\vec{T}_b)$ for the rain \vec{R} given brightness temperatures \vec{T}_b in terms of the more readily computable probability $p(\vec{T}_b|\vec{R})$ for the brightness temperatures given the rain :

$$p(\vec{R}|\vec{T}_b) = p(\vec{T}_b|\vec{R}) \cdot p_{prior}(\vec{R}) \quad (1)$$

The main obstacle to conducting these studies is the large number of variables one has to account for. In section II we begin by studying the vertically stratified rain by itself, in order to derive an economical representation of the rain profiles. In section III we study the brightness temperatures and derive expressions for the conditional covariances on both sides of (1). In section IV, we further use our results to derive first-order parametrized retrieval formulas that estimate rain rates and their uncertainties from measured brightness temperatures.

II. PRINCIPAL COMPONENT ANALYSIS OF THE VERTICAL RAINFALL R

The passive-microwave TRMM database represents rain profiles by stratifying the atmosphere into 14 homogeneous layers, of which 8 are below the typical 4.5km freezing level in the tropics. This implies that one would require at least eight variables to describe the liquid rain for each profile. A principal value analysis reveals that this number can be reduced. Indeed, calling R_1, \dots, R_8 the rain in the first eight 0.5-km layers above the surface (numbered from the surface up), one can compute the covariance matrix of these variables from one's database, and diagonalize it : the matrix of change of basis specifies which eight (new) linear combinations of the R_i 's are mutually uncorrelated, and the associated eigenvalues determine the amount of information carried by each of the new variables : large eigenvalues indicate a correspondingly large variation in the associated variable, while smaller eigenvalues indicate that the value of the corresponding variable changes relatively little over the whole data. In practice, we calculated the covariance matrix of $\log(R_i)$ for the TRMM cloud-simulations database, then diagonalized it. The main result is that the largest eigenvalue is significantly larger than the remaining seven, and its eigenvector is very close to $R'_1 \simeq \frac{1}{\sqrt{8}} \sum_1^8 \log R_i$. The eigenvalues were

$$45 > 0.51 > 0.054 > 0.0024 > \dots > 3.4 \cdot 10^{-6}$$

suggesting that the last seven eigenvariables

$$R'_2 = 0.38R_1 + 0.35R_2 + 0.26R_3 + 0.15R_4 + 0.006R_5 - 0.18R_6 - 0.41R_7 - 0.67R_8 \quad (2)$$

$$R'_3 = -0.5R_1 - 0.29R_2 + 0.03R_3 + 0.31R_4 + 0.454R_5 + 0.37R_6 + 0.04R_7 - 0.47R_8 \quad (3)$$

$$R'_4 = 0.47R_1 - 0.08R_2 - 0.46R_3 - 0.38R_4 + 0.043R_5 + 0.42R_6 + 0.34R_7 - 0.35R_8 \quad (4)$$

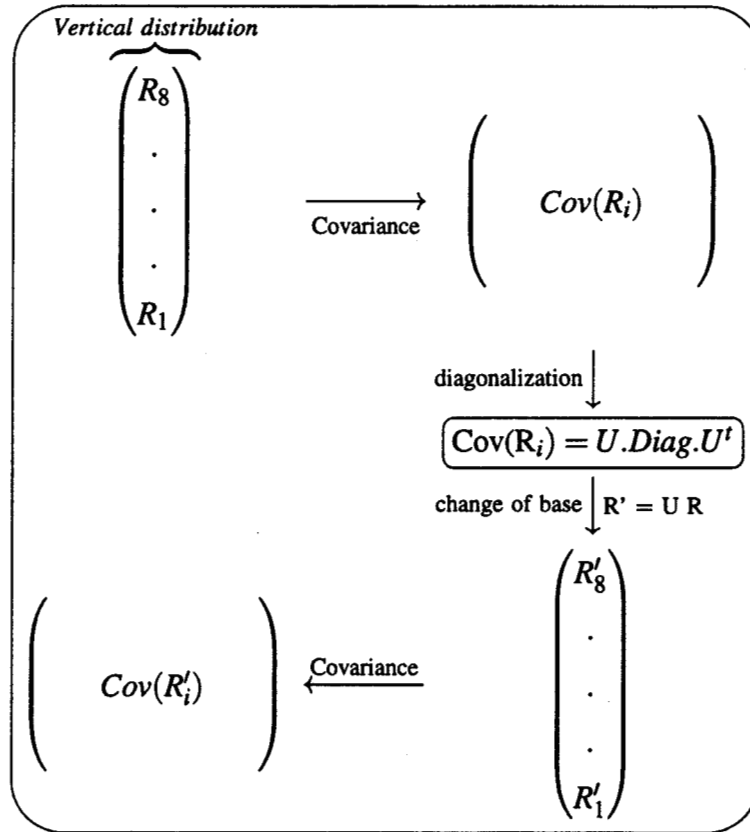
$$R'_5 = -0.4R_1 + 0.50R_2 + 0.28R_3 - 0.28R_4 - 0.374R_5 + 0.11R_6 + 0.44R_7 - 0.24R_8 \quad (5)$$

$$R'_6 = 0.21R_1 - 0.46R_2 + 0.19R_3 + 0.40R_4 - 0.35R_5 - 0.31R_6 + 0.53R_7 - 0.20R_8 \quad (6)$$

$$R'_7 = -0.1R_1 + 0.38R_2 - 0.52R_3 + 0.19R_4 + 0.367R_5 - 0.55R_6 + 0.31R_7 - 0.07R_8 \quad (7)$$

$$R'_8 = 0.06R_1 - 0.23R_2 + 0.45R_3 - 0.57R_4 + 0.513R_5 - 0.35R_6 + 0.16R_7 - 0.04R_8 \quad (8)$$

could be considered constant without incurring a very large error in the description of the rain : the vertical distribution of rain in the atmosphere could thus be described to first order by the vertically averaged rain rate R'_1 and the constant values of the means of R'_2, \dots, R'_8 .



Indeed, when reconstructed using R'_1 and the mean values $\mathcal{E}\{R'_2\} = 0.0635$, $\mathcal{E}\{R'_3\} = 0.0432$, $\mathcal{E}\{R'_4\} = -0.003$, $\mathcal{E}\{R'_5\} = -0.0002$, $\mathcal{E}\{R'_6\} = -0.0001$, $\mathcal{E}\{R'_7\} = 0.00004$, $\mathcal{E}\{R'_8\} = 0.00007$, the values for the rain rates were within 24% of the original values. Table I shows the individual results for each of the eight layers, and figure 1 illustrates the case of the near-surface layer.

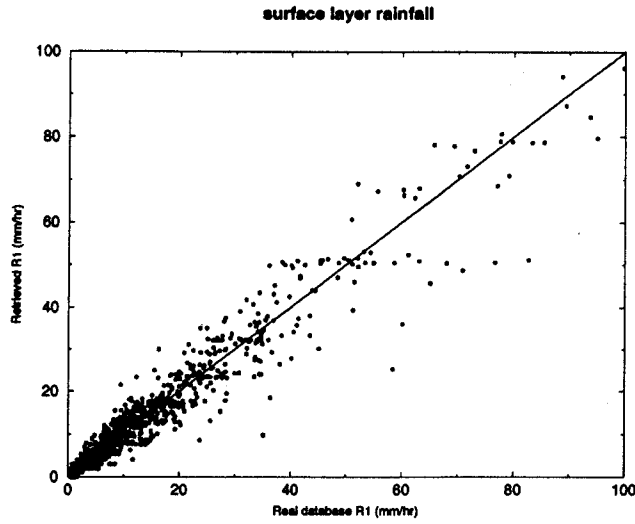


Fig. 1. Retrieved surface layer R_1 from R'_1 and R'_2 .

In order to verify that this high correlation between the rain in the various layers is not due to an artifact of the cloud models used to generate the TRMM passive-microwave database in the first place, a similar analysis was applied to actual data from the TRMM radar. We analyzed the data from sixty orbits performed in september 1998. The natural logarithms of the rain-rate estimates of the TRMM combined algorithm ([1]) for the fourteen 250m-layers between 750m and 4km were used. The first three altitude bins near the surface were ignored to avoid surface clutter problems. The covariance matrix was calculated and diagonalized. The results obtained are quite similar to the ones found for the passive microwave database rain rates. For convective

	rms deviation (mm/hr)	relative deviation (%)
R_1	1.2675	12.99
R_2	1.1499	11.27
R_3	0.8296	8.35
R_4	0.5173	6.03
R_5	0.4205	5.39
R_6	0.6077	7.31
R_7	0.9812	13.07
R_8	1.3320	23.63

TABLE I

RMS error on the rainrate estimated for each layer from the mean rainrate R'_1 , R'_2 and $\mathcal{E}\{R'_3\}, \dots, \mathcal{E}\{R'_8\}$.

events, the eigenvalues were $12.46 > 5.1 > 0.94 > 0.3 > \dots > 1.10^{-2}$. The coefficients of the eigenvector $\sum_i a_i \log(R_i)$ for the first eigenvalue 12.46 all verified $0.17 < a_i < 0.3$, quite close to the value $\frac{1}{\sqrt{14}} \simeq 0.267$. Hence R'_1 is indeed very close to be the vertically averaged rainfall. The eigenvalues in the stratiform case were similar to those in the convective case : $7.6 > 1.86 > 0.4 > 0.14 > \dots > 8 \cdot 10^{-3}$. The coefficients of the eigenvector $\sum_i a_i R_i$ corresponding to the first eigenvalue were in the range $0.21 < a_i < 0.29$. Merging all cases together, the eigenvalues were $11.8 > 0.43 > 0.14 > \dots > 9 \cdot 10^{-3}$ with an eigenvector $\sum_i a_i R_i$ for the first eigenvalue satisfying $0.21 < (a_i) < 0.29$. As in the case of the passive-microwave database, the first eigenvalue is far bigger than the remaining ones, although, since we do have 14 layers, the second eigenvalue cannot be negligible. It is particularly interesting to note that for the convective, stratiform, or all merged events, the eigenvector $\sum_i b_i R_i$ for this second eigenvalue always had the form $(b_1, \dots, b_7, -b_8, -b_9, \dots, -b_{14})$, with $0.13 < b_1, \dots, b_6, b_9, \dots, b_{14} < 0.34$ and $b_7 \cong b_8 \cong 0.05$. In other words, the second eigenvector quantifies the difference between the rain below 2.25km and the rain above 2.75km. This is remarkably similar to the case of the TRMM cloud-simulations database : indeed, (2) specifies that the second eigenvector for the rain described in the database is the difference between the rain below 2km and the rain above 2.5km. Figure

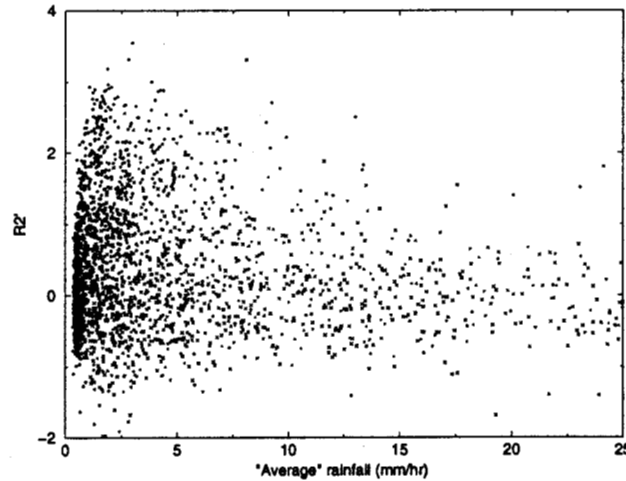


Fig. 2. R'_2 versus $\exp(R'_1/\sqrt{N})$, with $N=8$ for the database (\times) and $N=14$ for the TRMM radar (\bullet).

2 shows the scatter diagrams of the first two eigenvectors, in the case of the TRMM passive-microwave database and of some TRMM radar data obtained during ten orbits in january 1999. In both cases, the second eigenvector varies most (and is therefore most descriptive) for the moderate rain rates. This is consistent with the fact that near-surface evaporation can be significant especially under stratiform rain, a process which is best quantified by the difference between the rain aloft and the rain near the surface. In summary, our principal component analysis confirms that the TRMM passive-microwave database is consistent with measurements in the tropics, and suggests that, in the tropics, one should be able to describe the vertical distribution of rain

using two variables only : the mean rainrate (the first eigenvector) and the difference between the rain in upper and lower layers.

III. CONDITIONAL COVARIANCES OF R AND T_b

Because it is almost always impossible to find an exact match for a set of measured radiances in one's database, one must quantify the conditional covariances of the variables in the database in order to estimate the uncertainty in any rain retrieval based on the database. In the previous section, in the course of the principal component analysis, we verified that the joint behavior of the TRMM database rain rates at different heights is almost identical to that of the (independent) estimates of the TRMM radar. Before proceeding to the calculation of the conditional covariances, we must check that the TRMM database brightness temperatures are also consistent with the TRMM observations, which we did by analyzing the TMI data obtained during six orbits on october 17 and 18, 1998. For each of the 85.5GHz channels, we had 113,007 rain and 2,521,922 clear-air samples, while for each of the other (lower resolution) channels we had 64,338 rain and 1,253,154 clear-air samples. Figure 3 shows the 10.7GHz V-pol histograms of the measurements and of the

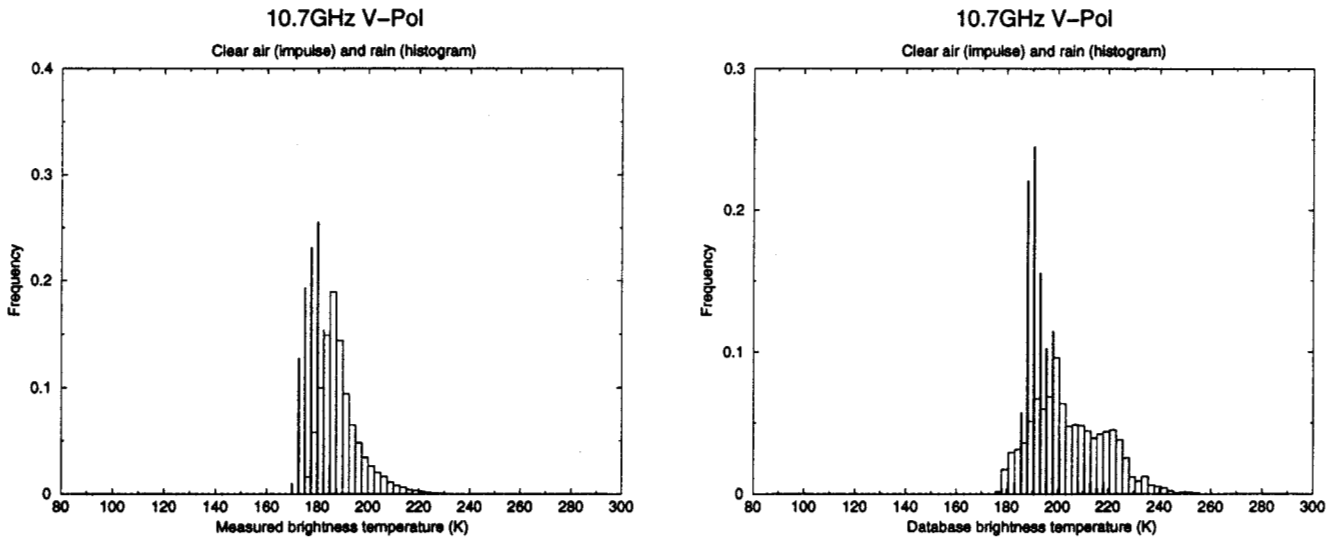


Fig. 3. Comparison of the 10.7GHz histograms of T_b .

database samples, for no-rain events as well as for rain cells. Since the database does not contain any “clear air” samples per se, that histogram was constructed using those samples for which the rain rate did not exceed 0.25 mm/hr anywhere in the rainy column. This explains the small positive bias of the clear-air database histogram compared with the measurements. The rain samples however show remarkable agreement with the data. The same features are evident in the histograms for the 10.7-V, 19.3-H, 19.3-V and 22.2-V channels. At 37GHz (figure 4), the database contains a relatively small but significant number of rain samples with low associated brightness temperatures extending well below the clear-air values, while no measurements fell in

this region. This feature is more pronounced in the 85.5GHz (figure 5), where the database contains no rain samples with brightnesses exceeding the clear-air cases while the measurements actually peak in that region. This could be an indication that the database either over-represents high-scattering events or that scattering is over-estimated in the radiative transfer calculations. A test for goodness of fit for the 37-V data reveals that the (approximately χ^2) statistic

$$\sum_{i=1}^{14} \frac{([\# \text{ database samples}]_i - [\# \text{ measurements}]_i)^2}{[\# \text{ measurements}]_i}, \quad (9)$$

computed using a binning into 2.5K-intervals between 240K and 270K, has a value of 36.4, which for a χ^2 variable with 13 degrees of freedom is at the 99.91st percentile. While this value is not as small as one may have liked, it is not unreasonable given that the very large sample size greatly increases the penalty for a mismatch between observations and simulated temperatures, the mismatch being at least partly due to the questionable representativity of the observations themselves. Thus, on the whole, the database temperatures are not flagrantly inconsistent with the observations.

Figure 6 shows the conditional means $\mathcal{E}\{T_b|R'_1\}$ of the brightness temperatures given the “mean” R'_1 . Except for the 10.7GHz channels, the curves are almost horizontal. Figure 6 also shows the conditional r.m.s. deviations. For light rain, the 85.5GHz uncertainties are the highest, approaching 60K, followed by the 10.7GHz H-pol uncertainty of about 30K. As the rain increases the uncertainties initially drop, then increase again once the rain rate exceeds about 10 mm/hr. For large rain rates, the 85.5GHz uncertainties climb beyond 80 followed closely by the 37GHz σ 's. This is undoubtedly due to the effects of scattering from ice. The uncertainties in the other channels remain below 40K. Table II and figure 7, showing the correlation coefficients of the various channels given R'_1 , complete the description of the conditional covariance. The high

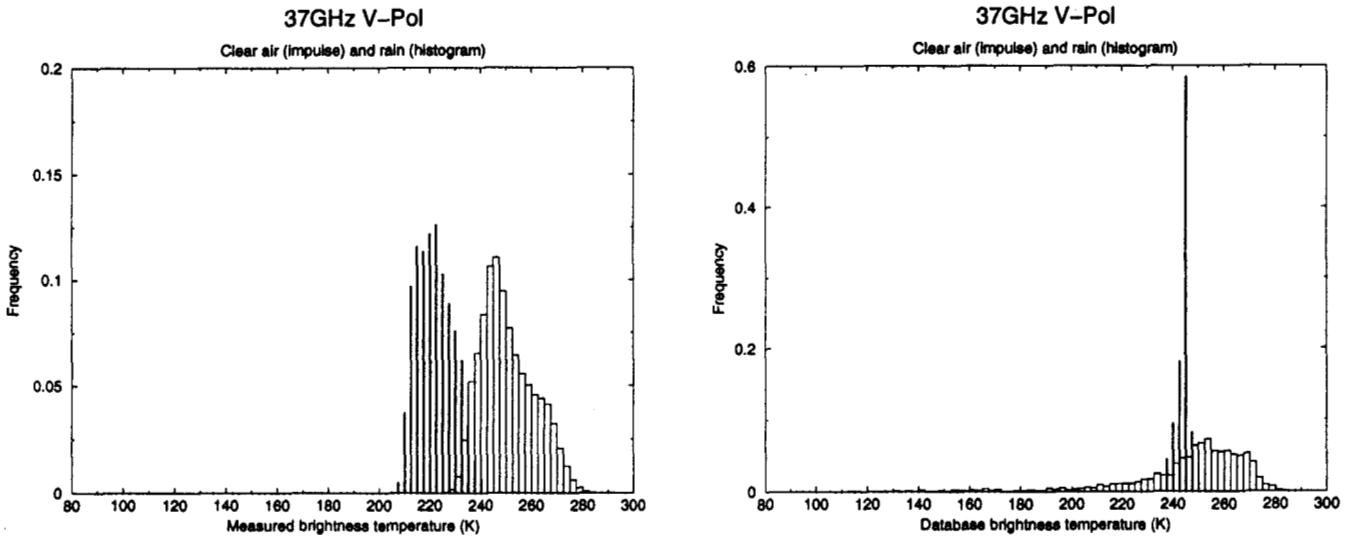


Fig. 4. Comparison of the 37GHz T_b histograms.

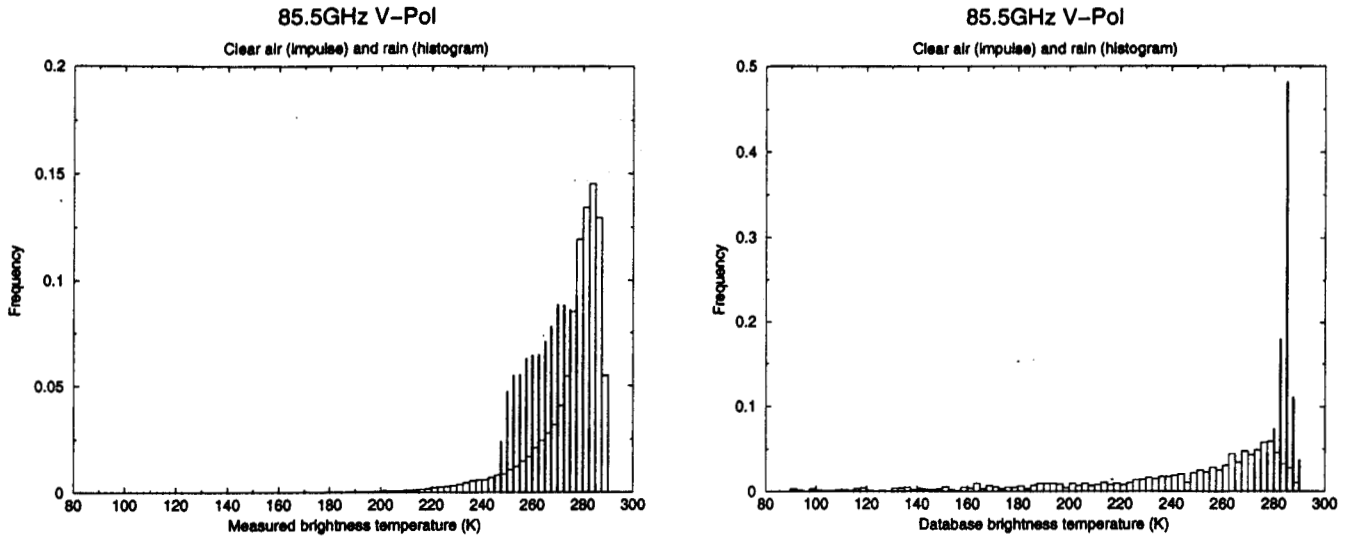


Fig. 5. Comparison of the 85.5GHz T_b histograms.

correlations between the two polarizations at each frequency are not surprising, since the forward radiative transfer model used to generate the database did not account for any polarization effects except those from the surface. Somewhat more surprising is the sign of the correlation coefficient between 19.3GHz H-pol and both 22GHz V-pol and 37GHz V-pol : for low rain rates the correlation is close to -1, but it becomes positive for rain rates above about 2.5 mm/hr and approaches +1 for high rain rates. More significant is the consistently positive correlation between 19.3GHz V-pol and the higher-frequency channels, and its relatively weaker correlation with the low-frequency channels. This suggests that, in the TRMM database, both 19.3GHz channels are affected by scattering in the cloud model used even at very low rain rates, the effect being more significant at V-polarization than at H.

To quantify the effect of the ambiguities in the database on the direct retrieval of the rain rates from mea-

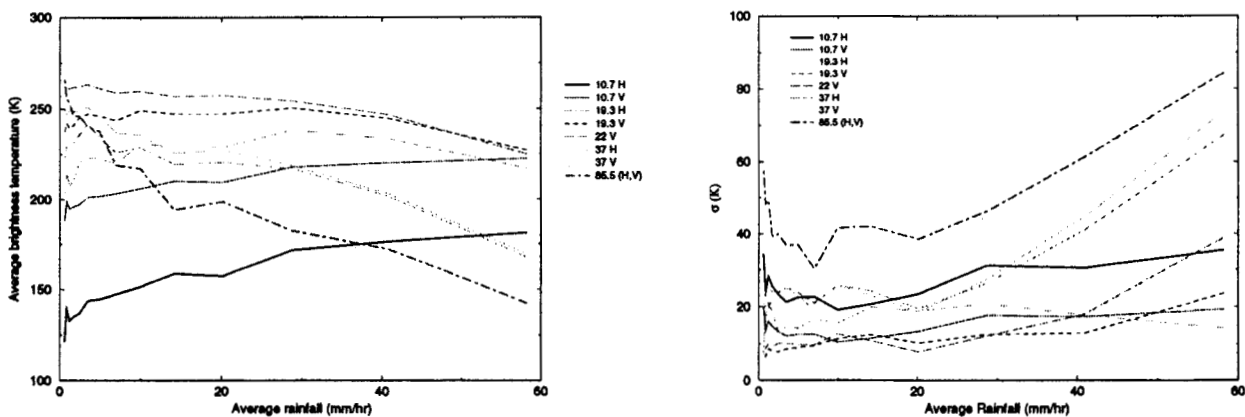


Fig. 6. Means and standard deviations of T_b given an "average" $R = \exp(R'_1/\sqrt{8})$.

	10.7V	10.7H	19.3V	19.3H	22.2V	37V	37H	85.5V	85.5H
10.7V	1	0.99	0.47	0.74	-0.45				
10.7H		1	0.43	0.72	-0.47				
19.3V			1	0.86	0.81		0.67		
19.3H				1					
22.2V				fig.7	1	0.86	0.88	0.70	0.74
37V	fig.7	fig.7	fig.7	fig.7		1	0.94	0.88	0.89
37H	fig.7	fig.7		fig.7			1	0.75	0.80
85.5V	fig.7	fig.7	fig.7	fig.7				1	0.99
85.5H	fig.7	fig.7	fig.7	fig.7					1

TABLE II

Correlation coefficients of T_b given R – most coefficients do not vary significantly with R .

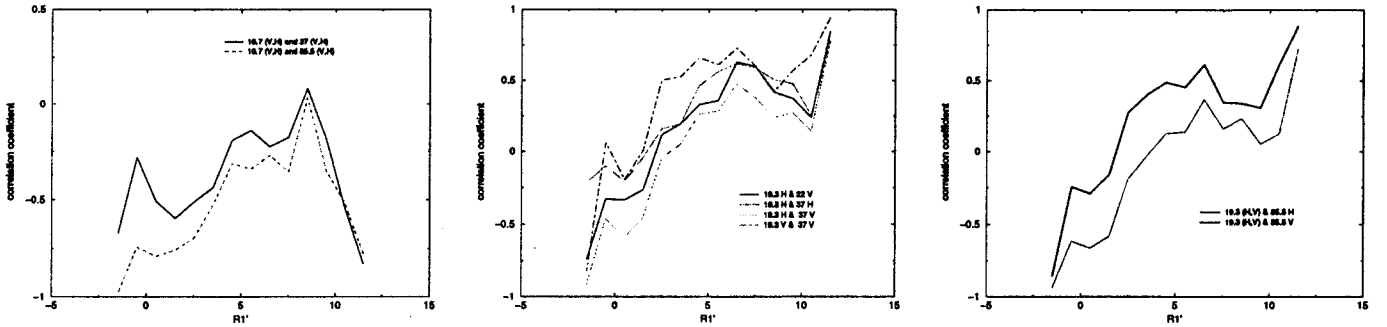


Fig. 7. Correlation coefficients for the passive channels given R_1' .

sured brightness temperatures, we proceed as before and start by reducing the number of variables required to describe the radiances. The eigenvalues of the covariance matrix of the database brightness temperatures turn out to be

$$5652 > 965 > 314.6 > 72.37 > 31.5 > 4.77 > 3.9 > 0.18 > 0.11 \quad (10)$$

with corresponding eigenvectors

$$T_1' = -0.13T_{10}^H - 0.07T_{10}^V + 0.03T_{19}^H + 0.08T_{19}^V + 0.15T_{22} + 0.3T_{37}^H + 0.37T_{37}^V + 0.6T_{85}^H + 0.6T_{85}^V \quad (11)$$

$$T_2' = 0.7T_{10}^H + 0.4T_{10}^V + 0.5T_{19}^H + 0.26T_{19}^V + 0.07T_{22} + 0.24T_{37}^H + 0.08T_{37}^V - 0.03T_{85}^H - 0.04T_{85}^V \quad (12)$$

$$T_3' = -0.42T_{10}^H - 0.2T_{10}^V + 0.2T_{19}^H + 0.265T_{19}^V + 0.34T_{22} + 0.45T_{37}^H + 0.3T_{37}^V - 0.3T_{85}^H - 0.36T_{85}^V \quad (13)$$

$$T'_4 = 0.3T_{10}^H + 0.1T_{10}^V - 0.57T_{19}^H - 0.35T_{19}^V - 0.2T_{22} + 0.45T_{37}^H + 0.4T_{37}^V - 0.135T_{85}^H - 0.17T_{85}^V \quad (14)$$

$$T'_5 = -0.1T_{10}^H - 0.256T_{10}^V + 0.4T_{19}^H - 0.2T_{19}^V - 0.7T_{22} + 0.41T_{37}^H - 0.2T_{37}^V + 0.05T_{85}^H - 0.007T_{85}^V \quad (15)$$

$$T'_6 = 0.47T_{10}^H - 0.8T_{10}^V + 0.1T_{19}^H - 0.2T_{19}^V + 0.25T_{22} - 0.1T_{37}^H + 0.06T_{37}^V - 0.01T_{85}^H + 0.002T_{85}^V \quad (16)$$

$$T'_7 = -0.06T_{10}^H - 0.007T_{10}^V + 0.2T_{19}^H + 0.024T_{19}^V - 0.4T_{22} - 0.5T_{37}^H + 0.7T_{37}^V - 0.1T_{85}^H + 0.02T_{85}^V \quad (17)$$

$$T'_8 = 0.16T_{10}^H - 0.27T_{10}^V - 0.37T_{19}^H + 0.8T_{19}^V - 0.33T_{22} + 0.04T_{37}^H - 0.06T_{37}^V - 0.1T_{85}^H + 0.1T_{85}^V \quad (18)$$

$$T'_9 = 0.02T_{10}^H - 0.05T_{10}^V - 0.04T_{19}^H + 0.14T_{19}^V - 0.07T_{22} - 0.08T_{37}^H + 0.06T_{37}^V + 0.7T_{85}^H - 0.7T_{85}^V \quad (19)$$

Once again, the eigenvalues decrease quite rapidly, the third one being already more than an order of magni-

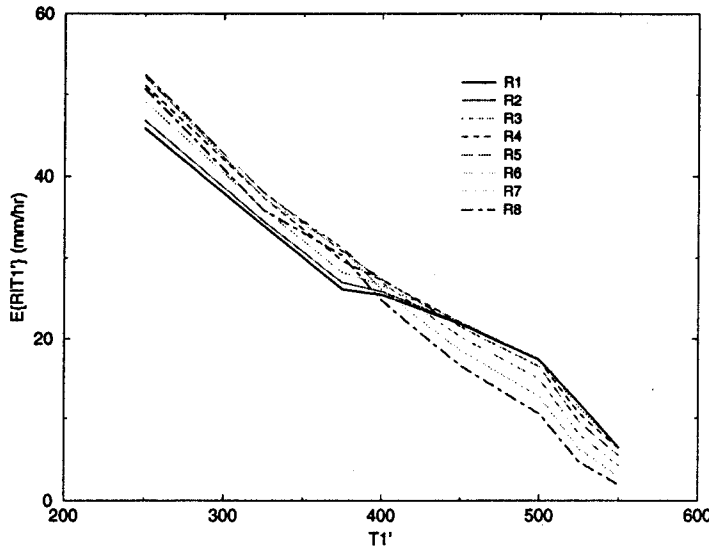


Fig. 8. Means of R given T'_1 .

tude smaller than the first. One can therefore quite adequately describe the 9 passive microwave measurements using T'_1 (and, for additional precision if required, T'_2) and the means of the remaining T'_i 's. Figure 8 shows the conditional mean of the R_i 's given T'_1 , and figure 9 shows the conditional standard deviations. As the figures show, the uncertainties do decrease as the rain itself decreases, but they increase as a proportion of the rain rate. Indeed, the standard deviations are consistently around 55% for the higher rain rates, then rise to about 65% when the rain rates drop to about 30 mm/hr, and continue rising as the rain drops, exceeding 100% as soon as the rain rates drop below 20 mm/hr and remaining near 15 mm/hr for the lowest rain rates. Since the rain rate remains positive, much of this deviation must necessarily lie above the mean, making an over-estimation of the rain likely if the joint behavior of the database radiances is not consistent with that of the measurements.

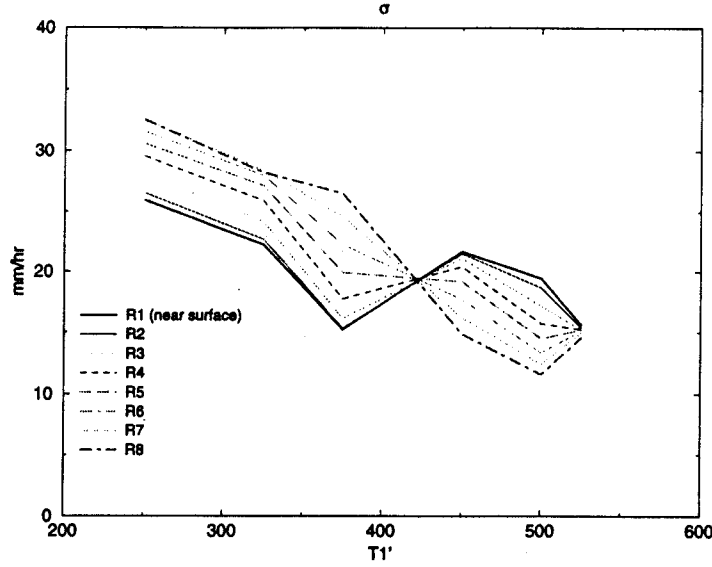


Fig. 9. *r.m.s. variation of R given T_1' .*

IV. ESTIMATION OF R USING MICROWAVE BRIGHTNESS TEMPERATURES T_b

The principal component analyses allowed us to reduce the number of variables required to describe the rain, as well as those required to describe the measured brightness temperatures. It is therefore natural to investigate the possibility of estimating the rain from the measured radiances directly using the reduced set of variances, without having to consult a database in real time. Since the vertical distribution of rain can be adequately described using a single variable R'_1 , the mean rainfall value in the atmosphere, the problem of estimating the rain from a vector of measured brightness temperatures can be reduced to estimating the corresponding value of R'_1 . For this application, we chose to consider a higher-resolution scenario than the previous case of TRMM, and used a cloud model simulation of a hurricane implemented on a 3km grid with 5 1-km rain layers and assuming a look angle of 52 degrees. We considered 9 channels : 10.7H, 10.7V, 19.3H, 19.3V, 21.3V, 37H, 37V, 85.5H and 85.5V.

In practice, it would be simplest to use a subset of all available microwave channels to estimate R'_1 , and thus “distill” the information contained in the database into a simple parametrized functional relation. Using an approach similar to the principal component analysis above, we looked for the “optimal” linear combination of the passive channels that will “best” estimate the rain, and quantify the residual ambiguity. Because the problem of finding the best relation between R'_1 and a combination T' of brightness temperatures T_i among 10.7GHz, 19.3GHz, 21.3GHz, 37GHz and 85.5GHz is a priori non-linear, we modify it slightly by trying to maximize the correlation’s numerator $E\{R'_1 \cdot T'\}$ keeping $E\{T'^2\}$ constant. This in effect minimizes the scatter between T' and R'_1 . Once the coefficients of T' are found, one can easily compute the mean and

variances of R' given T' , and thus determine the inverse relation and its uncertainty.

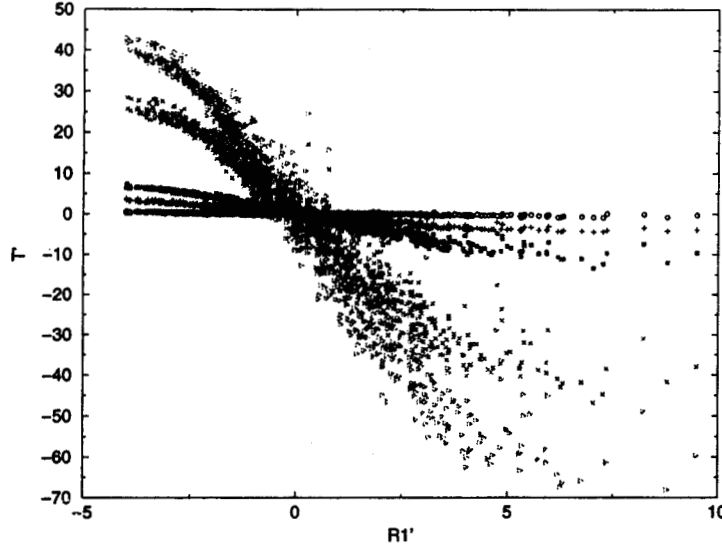


Fig. 10. Selected candidate T' 's : T'_{opt} using 4 H-pol with 21.3V (\triangleright); all 5 V-pol (\times); 4 H-pol with 19.3V (\blacksquare); 4 H-pol with 10.7V ($+$); 19.3V, 19.3H, 21.3V, 37H and 85.5H (\circ).

Figure 10 shows the optimal combination T'_{opt} plotted against the “mean” R'_1 ,

$$T'_{opt} = 0.41 T_{10.7H} + 0.36 T_{19.3H} + 0.79 T_{21.3V} - 0.18 T_{37H} - 0.182 T_{85.5H} \quad (20)$$

along with selected suboptimal candidate T' 's. The r.m.s. uncertainty corresponding to T'_{opt} is about 26.44%. As figure 10 shows, the best combination omitting the 10.7GHz channels gives a flat plot with a σ of more than 50 %. The result without the 19.3GHz channels is not very good either.

Using T'_{opt} , the rain-retrieval results are rather encouraging. Figure 11 shows R'_1 versus T'_{opt} . There is manifestly little scatter around the diagonal. Indeed, the r.m.s. uncertainty in the R'_1 estimates is about 9%. Finally, figure 12 shows the T'_{opt} -reconstructed near-surface rain rate R_1 plotted against the original R_1 , and figure 13 shows the results of the reconstruction for each of the remaining 4 layers R_2, \dots, R_5 . Table III gives the precisions of retrieved R_i in each layer. These results are quite encouraging.

V. CONCLUSION

Our study of the joint behavior of the rain in a horizontally stratified atmosphere and the associated microwave radiances shows that the single most crucial variable characterizing the rain profile is the vertically averaged rain rate, followed as a distant second by the difference between the high-altitude sub-freezing-level rain and the precipitation closer to the surface, the remaining rain eigen-variables having negligibly small variances implying that they can safely be considered constant (equal to their respective means). The mea-

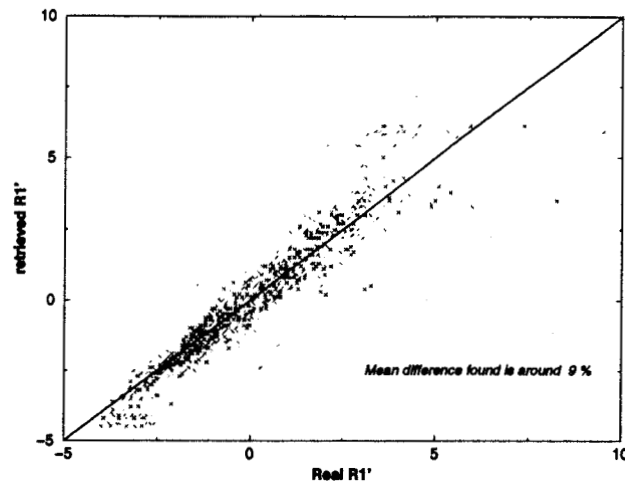


Fig. 11. R_1' , retrieved from T_{opt}' , versus the actual R_1' .

	rms deviation (in mm/hr)	error (in %)
R_1	± 4.35	41.1
R_2	± 3.25	29.8
R_3	± 2.12	22.7
R_4	± 2.27	36.3
R_5	± 1.48	54.4

TABLE III

Error in the rainrate calculated for each layer using the mean rainrate R_1' estimated from T_{opt}' and using $E\{R_2'\}, \dots, E\{R_5'\}$

measurements of the passive microwave channels can similarly be described using two linear combinations of the brightness temperatures. The conditional standard deviation of the rain rates given these eigen-radiances is a nearly linear function of the conditional mean rain rate when the latter is high, equal to about 55% of the rain rate, but the proportion rises to 65% when the rain is around 30 mm/hr, and exceeds 100% when the rain drops below 20 mm/hr. The study also shows that for a higher-resolution situation such as the case of an airborne sensor, the vertical rain rates can be adequately estimated using five of the TRMM passive microwave channels and an associated database similar to that used for TRMM, with an r.m.s. uncertainty (due to the variations accounted for in the model database) below 55%.

ACKNOWLEDGMENTS

Svetla Veleva is gratefully acknowledged for several helpful discussions. This work was performed at the Jet Propulsion Laboratory, California Institute of Technology, under contract with the National Aeronautics

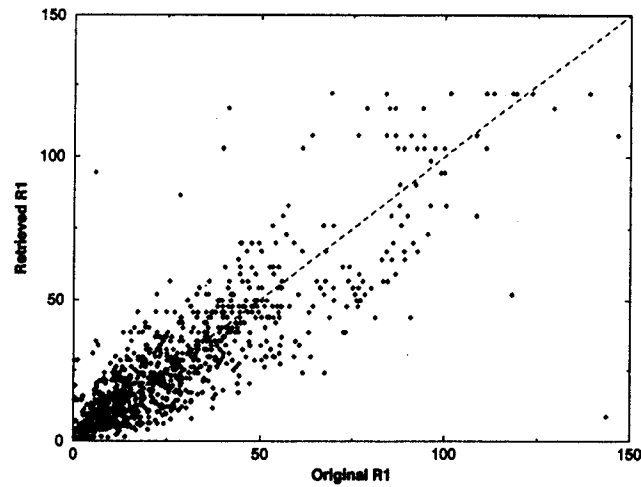


Fig. 12. R_1 , retrieved from T_{opt}^i and $E\{R_2^i\}, \dots, E\{R_5^i\}$, versus the actual R_1^i .

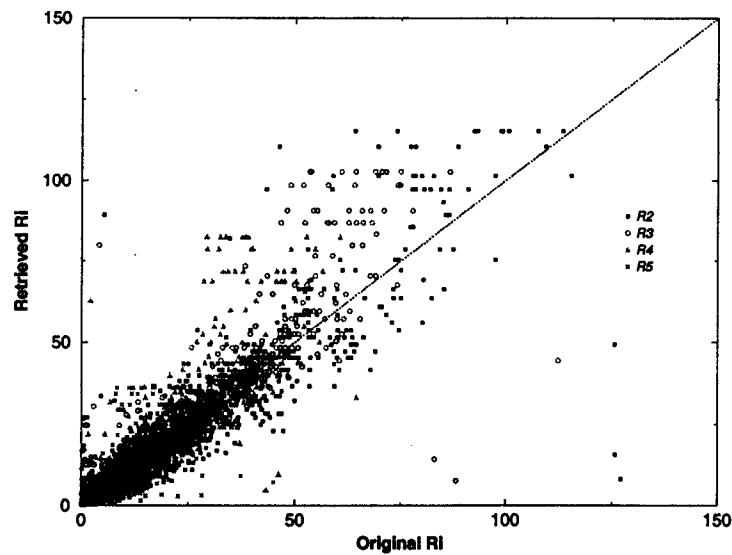


Fig. 13. R_i , retrieved from T_{opt}^i and $E\{R_2^i\}, \dots, E\{R_5^i\}$, versus the actual R_i^i 's.

and Space Administration.

REFERENCES

- [1] Z.S. Haddad, E.A. Smith, C.D. Kummerow, T. Iguchi, M.R. Farrar, S.L. Durden, M. Alves and W.S. Olson, *The TRMM 'Day-1' radar-radiometer combined rain-profiling algorithm*, J. Met. Soc. Japan, vol. 75, no. 4, pp 799-809, 1997.
- [2] C.D. Kummerow, W.S. Olson, L. Giglio, *A Simplified Scheme for Obtaining Precipitation and Vertical*

- Hydrometeor Profiles from Passive Microwave Sensors*, IEEE Tran. geosc. remote sensing, vol. 34. no. 5, pp 1213-1232, September, 1996.
- [3] C.D. Kummerow and L. Giglio, *A Passive microwave Technique for Estimating Rainfall and Vertical Structure Information from Space. Part I : Algorithm Description*, J. Appl. Meteo., vol. 33, pp 3-18, January, 1994.
- [4] C.D. Kummerow and L. Giglio, *A Passive microwave Technique for Estimating Rainfall and Vertical Structure Information from Space. Part II : Applications to SSM/I Data*, J. Appl. Meteo., vol. 33, pp 19-34, January, 1994.
- [5] S.-T. Soong and W.-K. Tao, *A numerical study of the vertical transport of momentum in a tropical rainband*, J. Atmos. Sci., vol. 41. no. 5, pp 1049-1061, 1984.
- [6] A. Mugnai, E.A. Smith and G.J. Tripoli, *Foundations for statistical-physical precipitation retrieval from passive microwave frequencies. Part II : Emission-source and generalized weighting-function properties of a time-dependent cloud-radiation model*, J. Appl. Meteo., vol. 32, pp 17-39, 1993.
- [7] E.A. Smith, A. Mugnai, H.J. Cooper, G.J. Tripoli, X. Xiang, *Foundations for statistical-physical precipitation retrieval from passive microwave frequencies. Part I : Brightness-temperature properties of a time-dependent cloud-radiation model*, J. Appl. Meteo., vol. 31, pp 506-531, 1992.
- [8] J. Tesmer and T.T. Wilheit, *An Improved Microwave Radiative Transfer Model for Tropical Oceanic Precipitation*, J. Atmos. Sciences, vol. 55, pp 1674-1688, 1998.